Tribology International 190 (2023) 109018

Contents lists available at ScienceDirect

Tribology International

journal homepage: www.elsevier.com/locate/triboint

Investigation on the role of the finger Transfer Function in tactile rendering by Friction-Induced-Vibrations

Livia Felicetti [a,b,*], Eric Chatelet [b], Benyebka Bou-Saïd [b,c], Antoine Latour [d], Francesco Massi [a]

[a] Department of Mechanical and Aerospace Engineering, Sapienza University of Rome, Italy
[b] Université de Lyon, INSA-Lyon CNRS UMR5259 LaMCoS, F-69621, France
[c] State Key Laboratory of Solidification Processing Northwestern Polytechnical University, Xi'an, Shaanxi, 710072, PR China
[d] Université Grenoble Alpes, CEA LITEN, Avenue des Martyrs 17, 38000 Grenoble, France

ARTICLE INFO

Keywords:
Finger transfer function
Tactile perception
Vibrotactile rendering
Biotribology

ABSTRACT

The world of haptics, tactile rendering of textures and tactile interfaces has witnessed significant expansion in the last years. When dealing with the design of tactile devices, the interaction between the device and the user's finger becomes crucial. With a focus on optimizing vibrotactile devices for texture rendering, a parametric analysis of the dynamic transfer function of the human finger was conducted under different test conditions. Discrimination campaigns have been conducted, exploiting an average transfer function among participants, to simulate surface textures by Friction-Induced Vibrations. The excellent results of the discrimination campaigns evidenced the effectiveness of the approach, allowing to get rid of the need to characterize the specific finger Transfer Function for each user of the vibrotactile device.

1. Introduction

In the vast panorama of sensory experiences that connect us to the external world, the sense of touch remains one of the most enigmatic and least comprehended. For decades, we have conquered the mastery of acoustic and sight stimuli, navigating the world of pressure and electromagnetic waves. Acoustic and visual interfaces have been integrated into our daily lives, becoming indispensable companions in our modern world, while, on the contrary, understanding the intricate mechanisms of tactile perception continues to elude our complete grasp. Artificially recreating touch, through tactile rendering of surfaces and textures, would allow to interact with virtual environments, feel the intricate details of fabrics and objects from a distance, or revolutionize surgical and tactile rehabilitation procedures through tactile feedback. Such advancements in haptics and tactile rendering could have a very strong social and technological impact, reshaping our perception of the world and the human-machine interfaces. Nevertheless, touch involves a complex interplay of the musculoskeletal sand proprioception systems, and it encompasses a wide range of mechanical stimuli, including forces, friction, vibrations, and temperature, among others, activating numerous types of mechanoreceptors.

In recent years, the development of tactile rendering devices has surged, exploring a variety of devices whose tactile feedback is based on different mechanical signals such as forces and vibrations [1–5]. Tactile devices utilizing modulation of friction have emerged as some of the most common approaches in this domain, based on different principles, mainly ultrasonic vibrations [6–12] and electro-vibrations [13–18]. In fact, friction has emerged as one of the most important mechanical stimuli (along with vibrations) in the mechanisms underlying tactile perception [6–8]. In the panorama of the most common rendering techniques stands also vibrotactile rendering, which is achieved by evoking tactile sensations through vibrations generated by different actuators and dynamic exciters [19–23]. A further objective is to combine various tactile feedback mechanisms, such as vibrotactile and friction modulation, into a singular device to fully simulate touch in its entirety. Ongoing efforts are underway to achieve this integration toward immersive tactile feedback [24–26]. When dealing with tactile devices, in most studies the contact between the user's finger (or hand) and the tactile device is mediated by a rigid tool or an object, both in the measurement phase and in the tactile rendering one [20,22–24,27,28]. In other studies, the user's finger is in direct contact with the device [29–31].

The sense of touch, by its nature, relies on the physical interaction with the object being explored. This principle holds true for tactile rendering as well, where the interaction between the tactile device and the user's finger plays a crucial role in designing effective systems.

* Corresponding author at: Department of Mechanical and Aerospace Engineering, Sapienza University of Rome, Italy.
E-mail address: livia.felicetti@uniroma1.it (L. Felicetti).

https://doi.org/10.1016/j.triboint.2023.109018
Received 29 August 2023; Received in revised form 23 September 2023; Accepted 8 October 2023
Available online 10 October 2023

Understanding and considering this essential aspect is a necessary step to develop tactile devices that can faithfully replicate touch. In this context, when mimicking the vibrational stimuli, it is of utmost importance to consider the dynamic response of the finger during its interaction with the device. By accounting for these dynamic aspects, designers could ensure the device delivers a realistic and immersive tactile experience, enhancing its usability and effectiveness in providing meaningful tactile feedback to the user.

In [13] the interaction between finger and touchscreen in a tactile device based on electro-adhesion has been investigated, evaluating the variation of the contact area and the friction coefficient at the interface. In [32] the finger transfer function has been characterized to investigate the vibration-induced injuries incurred by manual workers. In [33] a non-linear viscoelastic model of human fingertip tissue has been experimentally tested to describe the trend of finger impedance, in order to understand how the force is transmitted in the fingertip and thus predict the stimulation of mechanoreceptors. In [34] the finger transfer function has been characterized by a dynamic exciter and used to reproduce the signals of Friction-Induced Vibrations (FIV) measured on textured surfaces. In [19] the frequency response of the used device and finger pad has been characterized and used to correct the signal in vibrotactile rendering. In [35] the transfer function of the human finger has been characterized to obtain the tangential skin deformation while exploring surfaces with different textures.

On another hand, when considering texture rendering, the duplex theory of tactile perception identifies two distinct pathways for discrimination of textures: fine textures are perceived and discriminated through high-frequency vibrational stimuli generated by sliding contact, whereas for coarse textures quasi-static contact is sufficient [36–39]. This fundamental differentiation has spurred extensive research into Friction-Induced Vibrations (FIV) and their intricate relationship with tactile perception of fine textures, encompassing both descriptive and hedonistic aspects [40,41]. Numerous studies have explored FIV and their relevance in discriminating various textures with diverse topographies, ranging from periodic and isotropic textures [30,31,34,40–42] to textiles [43–46] and beyond [36,47–50], depending as well on the contact boundary conditions (sliding velocity, load etc) [51–53]. Additionally, researchers have delved into the brain's response to mechanical stimuli [10,54–56], further enhancing our understanding of the complex interplay between sensory inputs and cognitive processing in tactile perception.

The PIEZOTACT device, developed in previous works [30,31], is employed in the present study and relies on a vibrotactile texture rendering approach. It aims to artificially recreate the tactile sensation of fine surface textures by vibrational stimuli, wherein induced vibrations have been identified as one of the most significant cues for discrimination and perception. Despite its importance in tactile perception, the role of friction is not investigated in this work, which is specifically focused on the rendering of the sole vibrational stimuli arising from the exploration of different textures of similar material samples.

With the goal to enhance vibrotactile rendering devices, a parametric study of finger transfer function on a large panel of participants, varying normal force and finger-surface angle during contact, is here performed. The finger transfer functions are compared across participants and test conditions, revealing minimal differences and allowing calculate an average transfer function to be used as a unique input, participant and condition independent, for the tactile device. The use of such an average transfer function is directly validated through discrimination campaigns of real and simulated textures using the PIEZOTACT tactile rendering device. Since vibrotactile devices exploit the transfer function of the device and the participant's finger, to reproduce the vibration previously measured during the exploration of real textures, the use of a universal finger transfer function aims to optimize such devices by getting rid of the need to recalibrate the device for each individual user.

2. Materials and method

In the first instance, the methodology for measuring and simulating, the mechanical stimuli (in particular the FIV), by means of a tactile rendering device named PIEZOACT [30,31] is presented.

Subsequently, two different test benches are presented to characterize the transfer function of the human finger, by means of an electrodynamic shaker, and then the transfer function of the overall system consisting of the vibrotactile device and the human finger. In such a way, the role of the dynamics of the finger alone is investigated, and then the one of the overall system, accounting for both the device and the finger. Parametric analyses are performed on panels of participants in different contact boundary conditions. This step is essential for optimizing the mimicking of the effective FIV stimuli, which is the basis of the tactile rendering methodology by the vibrotactile device.

Finally, a discrimination campaign is performed on the real and simulated surfaces, using an average transfer function, averaged on both the contact parameters and the participants, to mimic the FIV stimuli measured when exploring real textures. The results from the discrimination campaign, obtained with the averaged transfer function, are then compared with discrimination campaigns carried on with the transfer functions specific to each participant.

2.1. Surface samples

A set of 13 surface samples with isotropic textures are used for this study. The samples have been obtained from sandpaper of different granulometries, starting from P40 up to P4000. The sample have been manufactured by silicon (ELKEM BLUESIL RTV 3428) moulds of sandpaper, in which an epoxy resin (Prochima E-30) has been then poured. Therefore, 13 square samples in epoxy resin have been obtained, with a side of 50 mm, which replicated the topography of the sandpapers. The manufacturing process and the topographic analysis of the samples are described into detail in [31]. The original sandpaper grade of the samples and the respective measured Ra roughness [31] are reported in Table 1 and the topographies are reported in Fig. 1. The used set of samples has been object of a previous work [31], in which the mechanical stimuli associated with tactile exploration (Friction-Induced Vibrations) were investigated and simulated by the tactile rendering device [30] [31].

2.2. Measuring and mimicking FIV stimuli

2.2.1. Measurement of mechanical stimuli during surface exploration

To measure the mechanical stimuli (Friction-Induced Vibrations and contact forces) associated with the active exploration of the real surfaces, the sample is fixed with double-sided tape on a triaxial force transducer (Testwell K3D60). An accelerometer (PCB 352A24, PCB Piezotronics, Inc.) is glued with wax on the nail of the participant's index finger. During the test, the participant maintains a contact force of

Table 1
Isotropic samples set characteristics.

Sample	# sandpaper	Ra [μm]
S1	P40	74.6
S2	P60	43.7
S3	P80	33.6
S4	P120	14.4
S5	P180	11.7
S6	P240	6.6
S7	P400	5.2
S8	P600	5.2
S9	P800	4.6
S10	P4000	4.5
S11	P2000	4.4
S12	P2400	4.3
S13	P1000	3.8

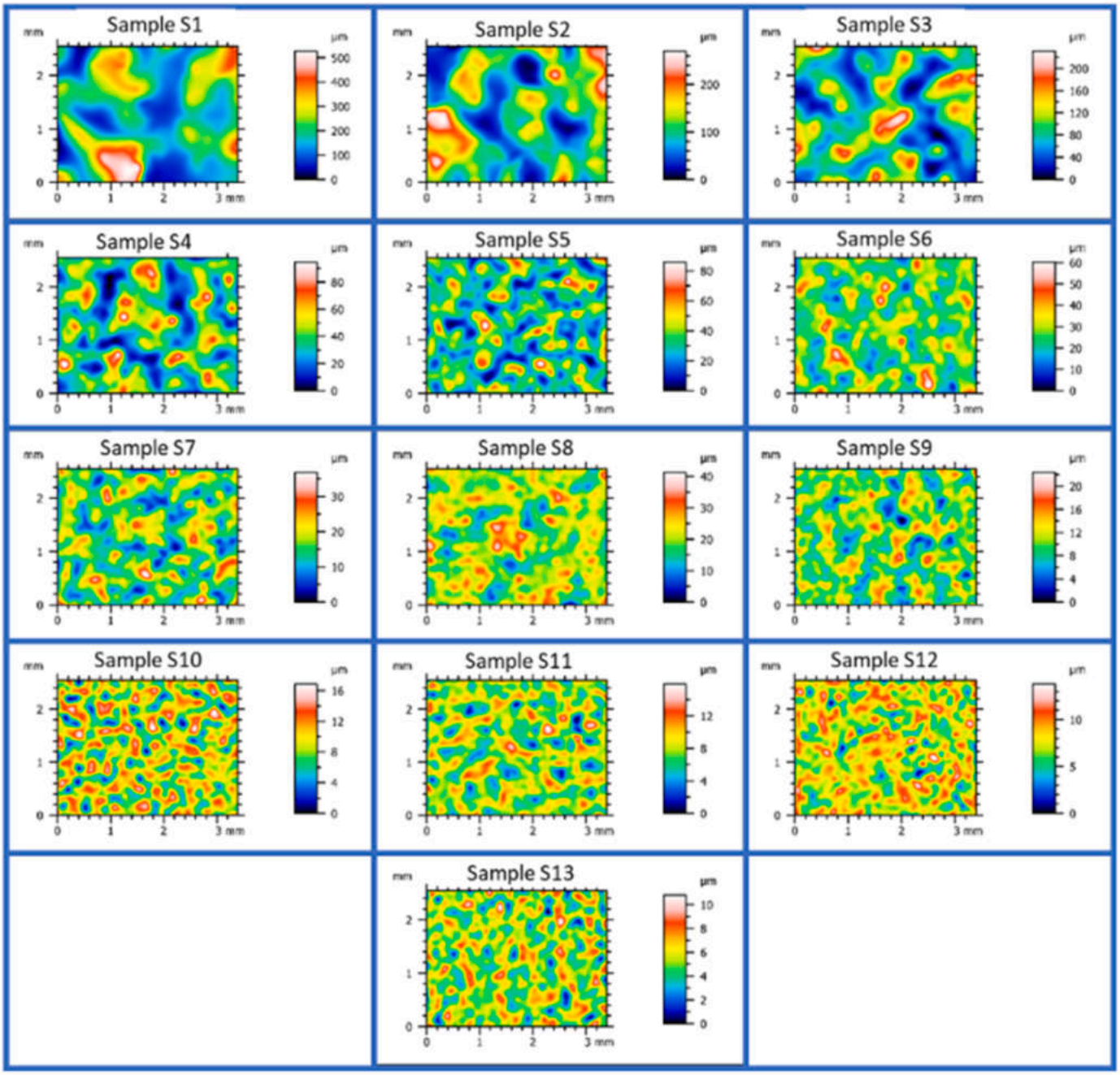

Fig. 1. Topographies of the isotropic samples obtained by the numerical microscope KEYENCE WHX 2000 [31].

approximately 0.2 N and a finger/surface angle of approximately 20 degrees, while sliding the finger against the samples (active touch), in proximal direction. The sliding velocity and the load are directly controlled by the participant, while actively exploring the surface. After a preliminary training, a minimum of 10 repetitions of the same exploratory movement are measured. The signals from the transducers are acquired by a SIRIUSi (DeweSoft) DAQ system at a 5 kHz sampling frequency. Fig. 2 shows the experimental setup to measure the mechanical stimuli elicited by the finger/surface sliding contact. A detailed analysis of the FIV signals from surface exploration and their correlation with surface discrimination are reported in a previous work [31].

The measurements of mechanical stimuli, according to the described protocol, have been carried out on 10 participants. These measures have been analysed and then used for the subsequent discrimination campaigns, by the mimicking technic described in the following.

2.2.2. *PIEZOTACT tactile device for tactile rendering*

A tactile device, named PIEZOTACT [30,31], is used to replicate the Friction-Induced Vibrations, previously measured when exploring the real surface samples. The tactile device is based on an electro-active polymer (EAP) piezoelectric actuator and its driving chain; it is able to actuate out-of-plane vibrations when a voltage is applied. The actuator is bounded into a PLA support, produced by additive manufacturing, and is driven by an electronic Texas Instrument (TI) card (Texas Instruments DRV2667EVM-CT), which is feed by an audio signal generated by a computer.

The aim is to reproduce, by the vibrotactile device, the FIV signals measured on the finger of the user when exploring the real textures. The main steps of the used tactile rendering technique, to correctly reproduce the FIV signals by the actuator, are the following:

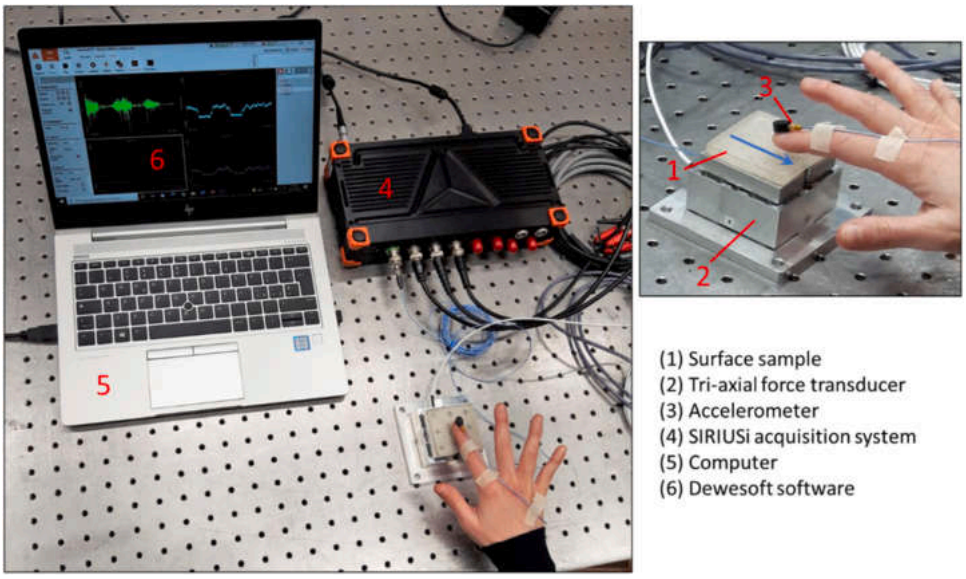

Fig. 2. Experimental setup to measure mechanical stimuli during tactile exploration.

- The FIV signal is preliminarily measured on the finger when exploring the real texture;
- A Fast Fourier Transform (FFT) is performed on the FIV signal;
- the FFT of the signal is divided by the overall electromechanical Transfer Function of the system (including the electrical circuits, the device and the finger);
- an inverse FFT is performed on the obtained spectrum to retrieve the time signal, which is then sent to the PIEZOTACT device.

The details of the development and validation of the PIEZOTACT device (shown in Fig. 3) and the texture rendering methodology can be find in [30,31].

2.3. Transfer Function estimation

Since the rendering methodology [30,31] is based on the processing of the target FIV signal by the Transfer Function of the whole electro-mechanical system, constituted by the combination of the PIEZOTACT device and the user's finger, its correct characterization assumes a fundamental role to correctly mimic the FIV signal.

Different users mean different fingers, placed on the actuator, with their proper transfer functions. Furthermore, being the system nonlinear, a role is also played by the contact parameters between the user's finger and the surface of the vibrotactile actuator, such as the normal contact force and the finger/surface angle. In previous works [30,31] the transfer function was re-characterized for each individual user; moreover, the contact boundary conditions between finger and actuator were maintained fixed for all the users.

With a view to optimizing the tactile device and the rendering methodology, a parametric analysis of the transfer function of the human finger, and then of the vibrotactile device including the user's finger, has been carried out on panels of participants.

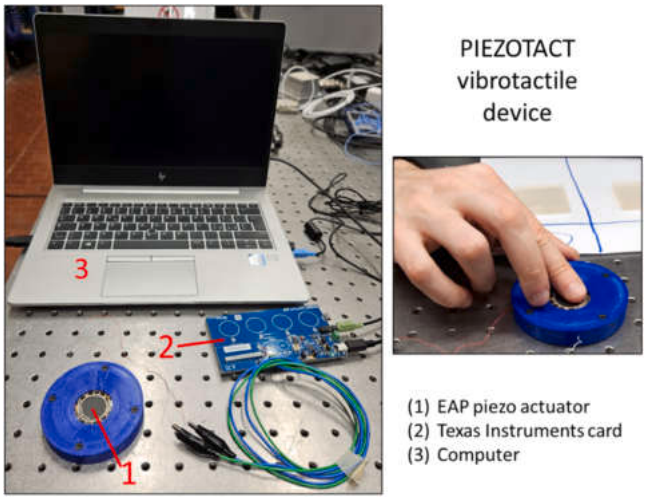

Fig. 3. The PIEZOTACT device.

2.3.1. Finger transfer function: experimental setup and protocol

A test bench (Fig. 4) has been developed to characterize the finger transfer function by means of a shaker (2075E The Modal Shop INC. A PCB Group CO., driven by the amplifier SmartAmp Power Amplifier 2100E21 The Modal Shop INC. A PCB Group CO.). The SIRIUSi DAQ system and the Dewesoft software are used both to acquire the signals from the transducers and to drive the shaker (via the amplifier), at a sampling frequency of 5KHz for all the input and output channels. An accelerometer (PCB PIEZOTRONICS 352A24) is fixed by wax on the fingernail of the participant to measure the acceleration. A piezoelectric charge force transducer (ENDEVCO 2321, driven by the amplifier Kistler KIAG SWISS Type 5001) is used to measure the contact normal force. This kind of force transducer allows to measure both the dynamic and the static components of the contact normal force, indispensable to perform the parametric analysis of the finger transfer function while monitoring the applied contact force. The force transducer is fixed on the top of the shaker. By its nature, this type of transducer is highly sensitive to temperature changes, which in this case are present due to the participant's finger temperature. To prevent temperature-induced drift, a ceramic plaque is glued to the force transducer to thermally and electrically insulate the force transducer from the participant's finger. A support for the participant's arm is set up to maintain an angle of approximately 20 degrees between the participant's finger and the contact surface. To experimentally characterize the finger transfer function, a random signal up to 1 kHz is delivered while the participant holds his finger on the force transducer, with the accelerometer on the fingernail. The transfer function inertance between the force and the acceleration is then calculated. The transfer function calculated in this way also considers the ceramic plaque between the force transducer and the finger. Nevertheless, the transfer function of the ceramic plaque,

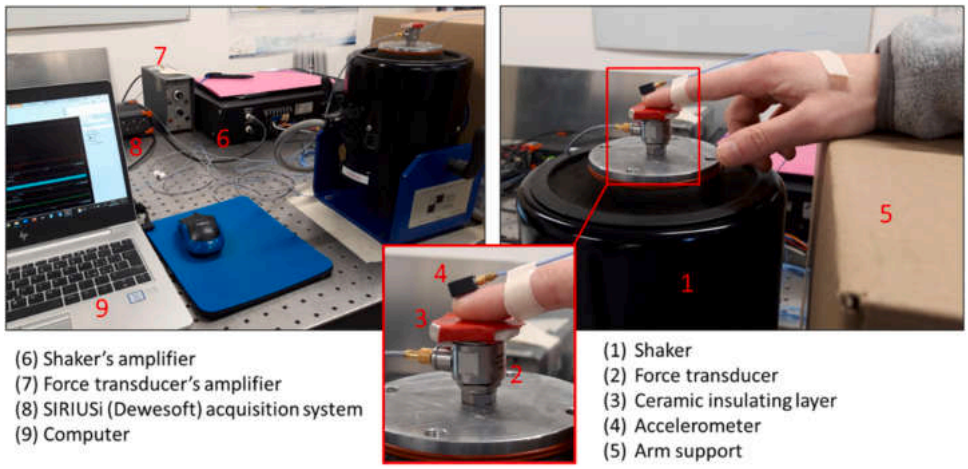

Fig. 4. Test bench for parametric analysis of finger transfer function.

characterized in a preliminary stage, is constant within the frequency range of interest, due to it high stiffness and has no relevant effect on the results.

The parametric study has been carried out on 5 participants (2 females and 3 males, ranging between 21 and 55 years). The angle between the finger and the ceramic surface has been set at 20 degrees, maintained by the configuration of the arm support. For each participant, measurements have been performed with a contact load of 0.2 N, 0.4 N and 0.6 N. The participant could hold the target contact load by observing the mean load displayed on the monitor.

2.3.2. *Overall electro-mechanical transfer function: experimental setup and protocol*

The vibrotactile device, including the participant's finger, has been subjected to a parametric analysis of the Transfer Function. Fig. 5 shows the exploited experimental setup. The actuator is fixed on a triaxial force transducer (Testwell K3D60) in order to monitor the contact force provided by the participant. An accelerometer (PCB 352A24, PCB Piezotronics, Inc.) is fixed on the participant's fingernail. A support is provided so that the participant's arm could rest during the measurement. The signals coming from the transducers are acquired using the SIRIUSi (Dewesoft) acquisition system at a sampling frequency of 5 kHz. The Transfer Function, obtained from the numerical input signal (random signal up to 1 kHz), sent via Matlab to the device, and the acceleration measured on the participant's fingernail is then characterized. Details on the methodology used to calculate the transfer function can be found in [30].

The parametric study was carried out on 20 participants (10 females and 10 males, ranging between 20 and 55 years). It is important to notice that the panel of participants who performed this campaign was composed by different participants with respect to the panel who performed the campaign described in Section 2.3.1.

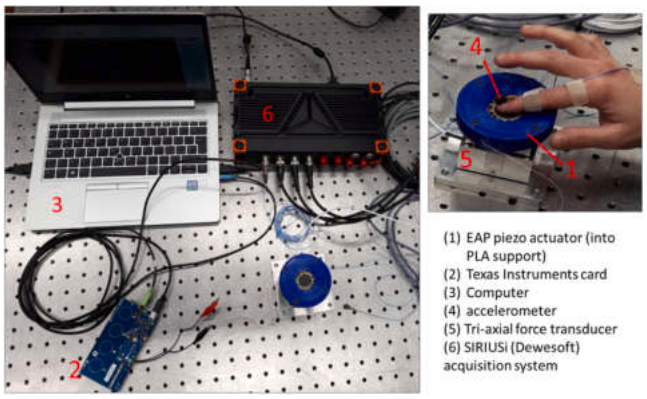

Fig. 5. Setup to characterize the transfer function of the PIEZOTACT device with the user's finger.

The parametric analysis has been conducted by varying the participant, the finger/actuator contact force and the finger/actuator inclination angle. As regards the contact force, the values of 0.2 N, 0.4 N and 0.6 N have been chosen (values in the range involved in tactile exploration). For the finger/actuator contact angle, the values of 20° and 40° have been selected. To assist the participant in maintaining the designated finger/actuator angle, the arm support has been conveniently arranged.

2.4. *Discrimination campaign*

A discrimination campaign, using the isotropic samples described in Section 2.1, has been performed on 10 participants (1 female and 9 males, with ages ranging between 24 and 45 years). The panel of participants who performed this campaign was composed by different participants with respect to the panels who performed the campaigns for the characterization of the Transfer Function described in Sections 2.3.1 and 2.3.2, and was as well different to the one who performed the discrimination campaign in [31]. This increases the robustness of the results.

Discrimination tests have been carried out on the real isotropic textures and on those simulated by the PIEZOTACT device, to evaluate the possibility to discriminate real and simulated surfaces on the basis of Friction-Induced Vibrations.

The average transfer function (see Section 3.2) has been used to process the FIV signal with the rendering method described in Section 2.2.2. Moreover, the used panel of participants to compute the average transfer function was not the same that performed the discrimination campaign.

The texture discrimination campaign is articulated into 3 different tasks (Fig. 6), described in the following.

2.4.1. *Task 1*

The first task (Fig. 6a) consists in sorting all the 13 isotropic samples in order, from the one perceived as the roughest to the one perceived as the smoother. The samples are randomly placed in front of the participant, who has to explore and sort them, relying only on the sense of touch.

2.4.2. *Task 2*

For each of the groups of 3 samples in Table 2, a discrimination task is performed on the real surfaces (Fig. 6b). The test consists in sorting the

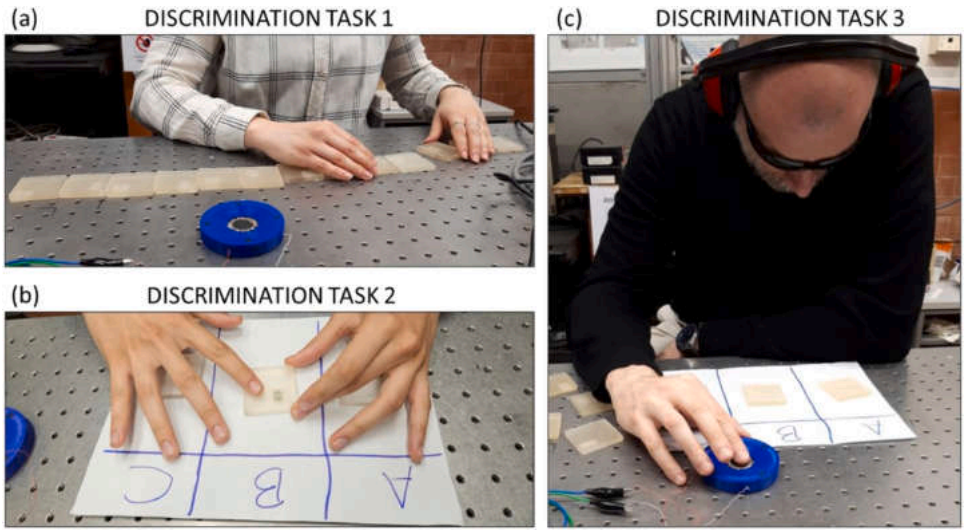

Fig. 6. Discrimination campaign, articulated into 3 different tasks: (a) TASK 1, sorting of the whole sample set; (b) TASK 2, discrimination of sets of real surfaces; (c) TASK 3, discrimination of sets of simulated surfaces by FIV reproduction.

Table 2
Used groups of isotropic samples for discrimination TASK 2 and 3.

GROUP	SAMPLES
A	S2, S4, S8
B	S5, S7, S9
C	S6, S11, S10
D	S1, S3, S13
E	S5, S8, S12
F	S5, S9, S10
G	S2, S3, S4
H	S1, S8, S13
I	S1, S7, S12
L	S4, S13, S10
M	S4, S8, S9
N	S13, S12, S10

3 samples in order from the roughest (placed in position A) to the smoother one (placed in position C).

2.4.3. TASK 3

For each of the groups of samples in Table 2, a discrimination task is then performed on the simulated surfaces by the PIEZOTACT device (processed with the average transfer function) (Fig. 6c). It is asked to the participant to place the finger on the actuator, and to perceive a sequence (containing the samples belonging to the group under examination) of the surfaces, simulated (mimicked FIV) with the vibrotactile device. By perceiving the only vibration signal sequence generated by the device, the participant has to declare the corresponding sequence of real surfaces (in term of A, B, C). In other words, at each signal reproduced by the actuator, and perceived by touching the actuator, the participant has to associate the corresponding real surface.

To perform TASK 2 and TASK 3, the samples are randomly divided into groups of 3, summarized in Table 2. During the campaign, participants are equipped with scratched glasses that allow to identify the shape and the position of the samples but not the texture, while earmuffs avoid acoustic feedback. No time limit is imposed to the participants to perform each discrimination task.

The same protocol and the same sets of samples, used in the present work, have been used in [31], in order to allow the comparison between the discrimination of real and simulated textures when the signal is processed with the specific transfer function of each participant (as in [31]) and the average transfer function (as in this work).

3. Results and discussion

In this section, first, the results of the parametric analysis on the finger transfer function, carried out using the two experimental protocols described in Section 2.3, are presented and discussed. Then, the FIV signals obtained by either the specific transfer function or the averaged one are compared with the original FIV, measured during the real surface exploration. Finally, the possibility of using an average transfer function among participants, to mimic the simulated surfaces using a vibrotactile device, has been tested by means of a discrimination campaign on real and simulated isotropic surfaces. The results of the discrimination campaign, using the average transfer function to obtain the simulated surfaces, are discussed in this section, and compared with the campaign performed in a previous work [31], in which the surfaces were simulated using the participant specific transfer functions.

3.1. Parametric analysis of finger transfer function

A parametric analysis of the finger transfer function has been carried on with the protocol described in Section 2.3.1.

Fig. 7 shows the comparison of the finger transfer functions among all the participants in the same test conditions: Fig. 7a reports the finger transfer function of all the participants with a normal contact load of 0.2 N, Fig. 7b with a contact load of 0.4 N and Fig. 7c with a contact load of 0.6 N. In all cases, the transfer functions of the participants are similar in trend and generate a bundle of curves of few dB of maximum deviation (less than 5 dB). Moreover, the maximum deviation of the curves presents a decreasing trend as the normal load increases. Fig. 8 presents the evolution of the maximum deviation as a function of the normal contact load. Increasing the contact load, the deviation of the transfer function with the participant decreases.

Fig. 9a presents all the curves relating to all the participants and all the test conditions (0.2 N, 0.4 N, 0.6 N) superimposed on the same graph, forming a bundle of curves with a similar trend and a maximum deviation of 8 dB.

An average transfer function among participants was then calculated for each test condition (normal load): an example of the average transfer function, superposed on the specific ones of the participants, is presented in Fig. 9b, for the case of a contact force of 0.2 N.

For each participant, the gain of the finger transfer function increases as the contact load increases; an example, referred to one participant, is reported in Fig. 10a. The same behaviour was found for all participants. For each test condition (0.2 N, 0.4 N, 0.6 N) the average transfer

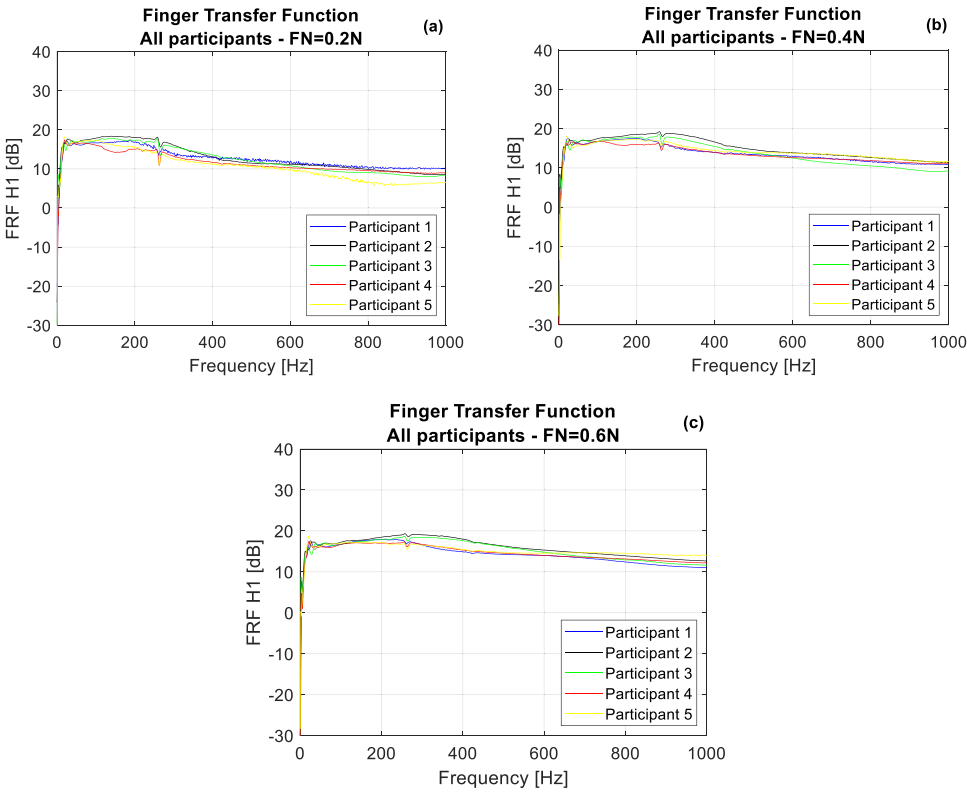

Fig. 7. Comparison, among all participants, of the finger transfer function in the same test condition: (a) contact load of 0.2 N, (b) contact load of 0.4 N, (c) contact load of 0.6 N.

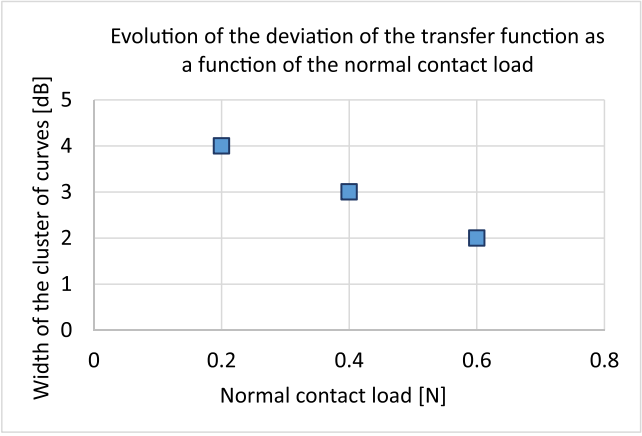

Fig. 8. Maximum deviation of the transfer functions as a function of the finger/actuator normal contact load.

function among all participants has been computed. Fig. 10b shows the comparison between the average transfer function among participants for the three test conditions (0.2 N, 0.4 N, 0.6 N). The trend of the average transfer function perfectly reflects the trend of the singular transfer function of each participant: as the normal contact load increases, the gain of the transfer function increases, due to the increase of the contact surface and mechanical coupling between fingertip and actuator..

The antiresonance at about 265 Hz, present in all figures, is characteristic of the used electrodynamical shaker. Being the aim of the study the comparison of the finger transfer functions of different participants and in different boundary conditions, always maintaining the same experimental setup, this resonance can be neglected.

In the light of the encouraging and consistent results of this preliminary campaign, investing the variability of the finger transfer function, a broader parametric analysis of the transfer function has been then performed directly on the vibrotactile rendering device, which is of interest for the processing of the FIV signals. In the campaign conducted on the device, the analysis has been extended to 20 participants, and further contact configurations, accounting for the overall electro-mechanical chain (PIEZOTACT and participant's finger).

3.2. *Parametric analysis of overall electro-mechanical transfer function*

A parametric analysis of the transfer function of the electro-mechanical system constituted by the electronics, the PIEZOTACT device and the user's finger has been carried on, with a panel of 20 participants and the protocol described in Section 2.3.2.

The parametric analysis was articulated in two points:

- For a single participant, the characterization of the finger transfer function is carried on by varying different contact parameters between finger and vibrating surface (contact force and finger/surface angle).
- For a given choice of contact parameters (contact force and finger/surface angle), the finger transfer function of different participants is compared.

The results, which agree with those found on the user's finger alone, and presented in Section 3.1, are listed in the following.

For each participant, fixed the finger/actuator angle, the gain of the transfer function increases as the contact force increases. The same trend is found for all the participants and for both the tested values of the finger/actuator angle (20° and 40°). Fig. 10 shows an example for a participant: whatever the finger/actuator angle, the transfer function increases as the contact force increases.

For each participant, fixed the value of the contact force, the transfer function referred to the two values of the finger/actuator angle (20° and

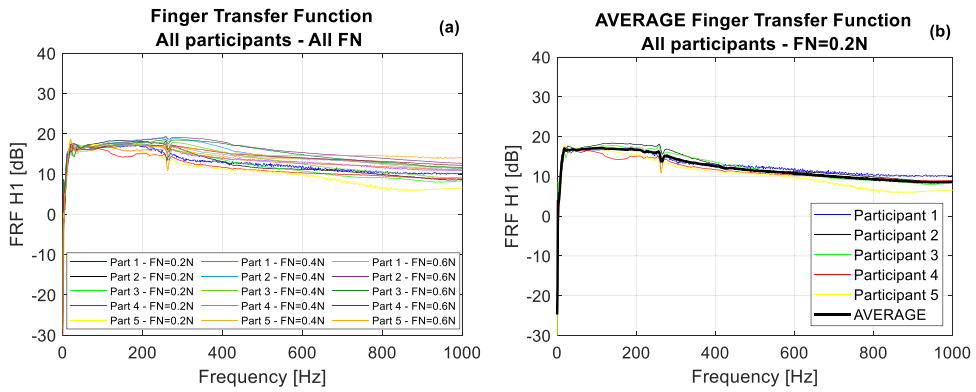

Fig. 9. (a) Comparison of finger transfer functions of all participants in all test conditions (0.2 N, 0.4 N, 0.6 N); (b) Example of calculated average transfer function among participants (for a load of 0.2 N) together with the specific participant curves.

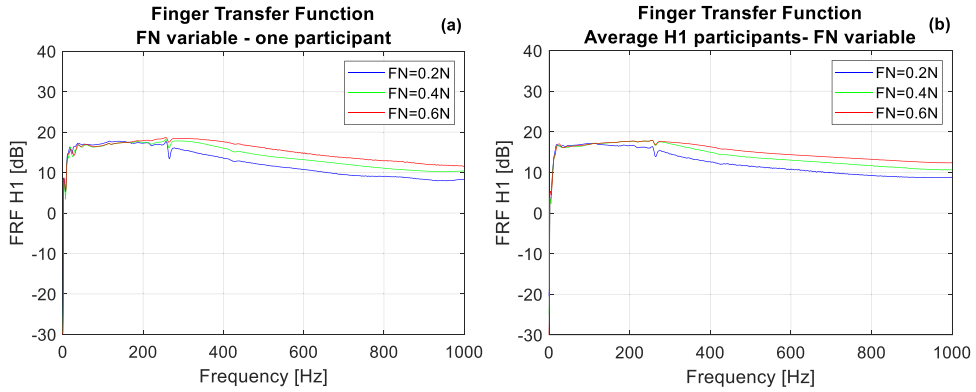

Fig. 10. (a) For one participant, the finger transfer function increases as the contact load increases. (b) average finger transfer functions, calculated among all participants, for each test conditions (0.2 N, 0.4 N, 0.6 N); the transfer function increases as the contact load increases.

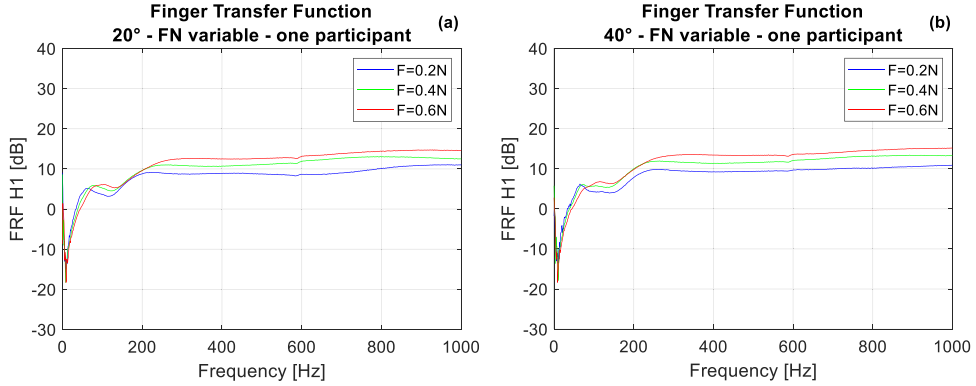

Fig. 11. Example of transfer function for a participant as the contact load varies, for an angle of 20° (a) and 40° (b).

40°) are compared. The variation of the angle causes a slight variation of the shape of the transfer function, but without a significant deviation and without a definite trend. This behaviour is found for all the contact forces and for all the participants. Fig. 12 reports an example for a participant.

Then, for each tested condition {angle, force}, the transfer functions of the 20 participants are compared. Fig. 13 shows an example for the condition {20°, 0.2 N}. As in Section 3.1, the transfer functions of all the participants form a bundle of curves with a few dB of maximum deviation, with a well-defined and repetitive trend. The average transfer function of all the curves is computed as well (see Fig. 13). The same behaviour is found for all test conditions {angle, force}. Fig. 14 reports the maximum deviation of the transfer functions of all participants for each test condition {angle, force}. Having fixed the finger/surface angle, the maximum deviation shows a decreasing trend as the contact force increases, for both 20° and 40°, with a maximum of 5 dB reached for the case {20°, 0.2 N}.

All the obtained transfer functions differ slightly between participants and within the tested ranges of contact boundary conditions. The real question lies on the effect of such slight variations on the mimicking of the FIV stimuli and on their perception by a subject, mediated by the stimuli transmission and elaboration by the brain. In the light of these results, it has been decided to use the average transfer function, calculate on the panel of participants, to simulate (mimic) the set of isotropic textures. A discrimination campaigns of the real and simulated isotropic surfaces has been then carried out. The average transfer function among

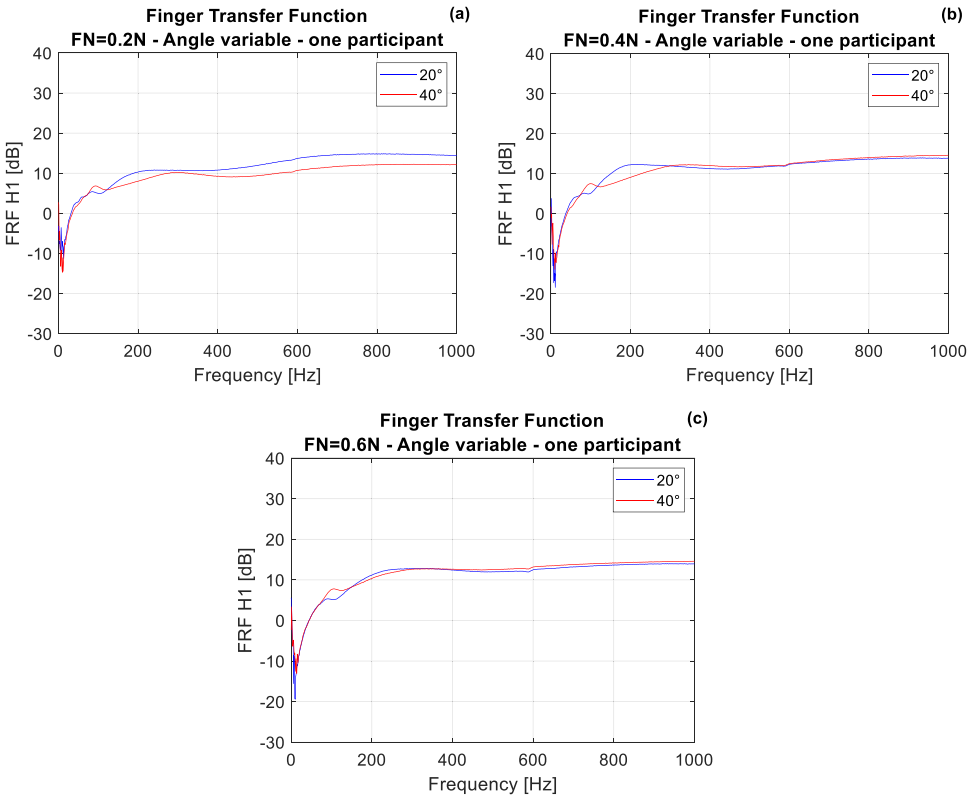

Fig. 12. Example of comparison, for a participant, between the transfer function for angles of 20° and 40° with a load of 0.2 N (a), 0.4 N (b), 0.6 N (c).

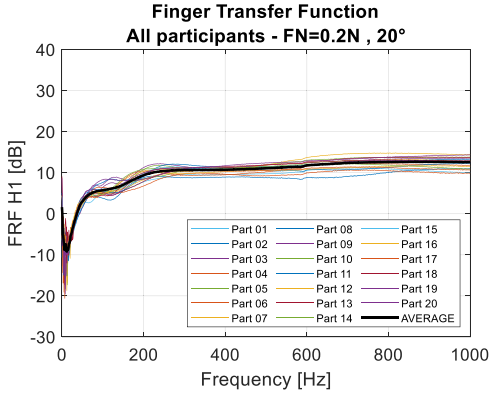

Fig. 13. Superimposition of the transfer functions of all the participants for the condition {20°, 0.2 N} and the average transfer function.

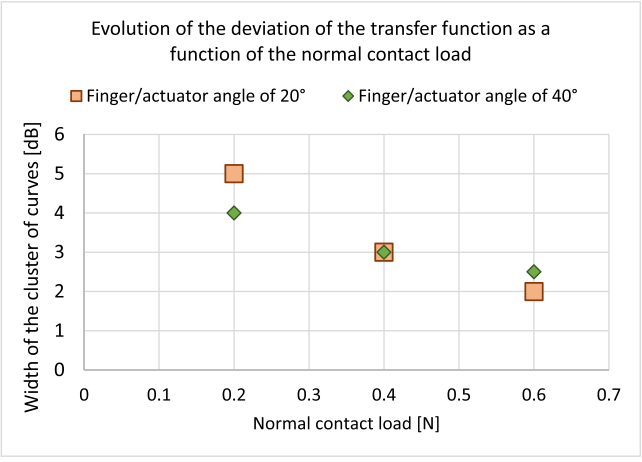

Fig. 14. Maximum deviation of curves, representing the transfer function of the system (PIEZOTACT device and user's finger) of all participants, as a function of the finger/actuator normal contact load and the finger/surface angle.

20 participants calculated for the combination {20°, 0.2 N} has been used (Fig. 12), as it reflects the choice of parameters with which the FIV were measured during the exploration of the real surfaces (see Section 2.2.1).

3.3. Validation of FIV signal rendering with average transfer function

As a preliminary step, the correct reproduction of the FIV stimuli using the PIEZOTACT device is verified both using the specific transfer function of the participants [31] and the averaged one. The FIV signal measured by exploring the real surface has been processed and sent to the device, while the participant placed his finger on the vibrating actuator and the acceleration was measured on the fingernail with the accelerometer. Fig. 15 shows the comparison between the PSD of the original FIV (red line), measured when the finger explores the real surface (S7), and the PSD of the signals measured during the reproduction of the signal by the vibrotactile device. The same original FIV signal has been processed in one case with the specific transfer function of one participant (blue line), and in the other case with the transfer function averaged among the participants (green line). When considering the specific transfer functions, the acceleration measured on the fingernail when exploring the surface are perfectly reproduced by the tactile device. In the case of the signal reproduced with the average transfer function, the reproduction is slightly less performing, but still well mimicking the main trend and amplitude distribution of the spectrum. In both cases, the real signal is well reproduced by means of the PIEZOTACT device on the participant's finger.

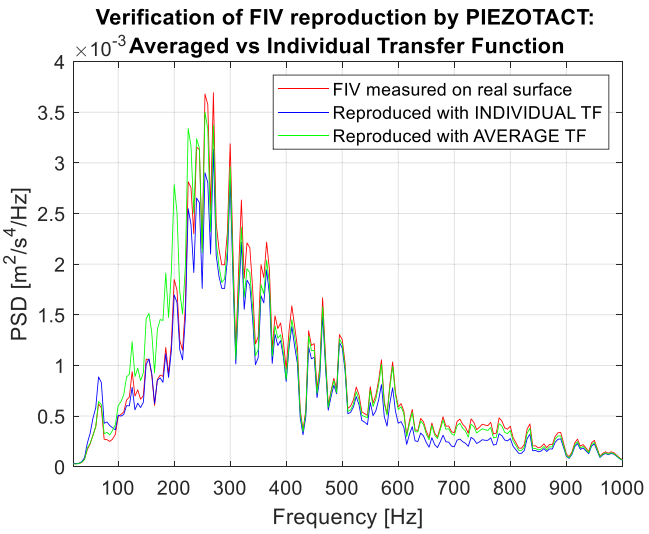

Fig. 15. Verification of reproduced FIV by PIEZOTACT device with individual and average Transfer Function.

3.4. Results of discrimination campaign of real and simulated isotropic surfaces using the average transfer function

The feasibility and effectiveness of using an average transfer function has been tested directly through a surface discrimination campaign. The discrimination campaign was carried out on 10 participants, on both the real and simulated surfaces, according to the protocol described in Section 2.4 and in [31].

To mimic the surface textures by the PIEZOTACT device, the average transfer function has been used (case {20°,0.2 N}, which corresponds to the conditions used during the exploration of the real surfaces).

The results are analysed by means of association matrices constructed as follows: on the horizontal plane of the matrix there are, on the abscissa axis x, the sample surfaces (real or simulated) presented to the participants, and on the ordinate axis y, the corresponding real sample sequence. In such a way, each pair {x,y} represents an association declared by the participant. The correct associations of the samples lie on the main diagonal of the matrix, while the discrimination errors lie outside the diagonal. The vertical axis presents the association percentages. These percentages are calculated as the ratio between the number of times that a particular association is declared by the participants and the number of times that the sample is presented to the participants among the whole tests, expressed as a percentage. Each matrix is cumulative of the associations declared by the full panel of participants. The same procedure for analysing the results was used in [30,31]. Fig. 16 shows the results of the discrimination campaign on both real and simulated surfaces: TASK 1 in Fig. 16a, TASK 2 in Fig. 16b and TASK 3 in Fig. 16c.

In all the three discrimination tasks, the association percentage on the main diagonal is very high for all the sample surfaces, which testifies

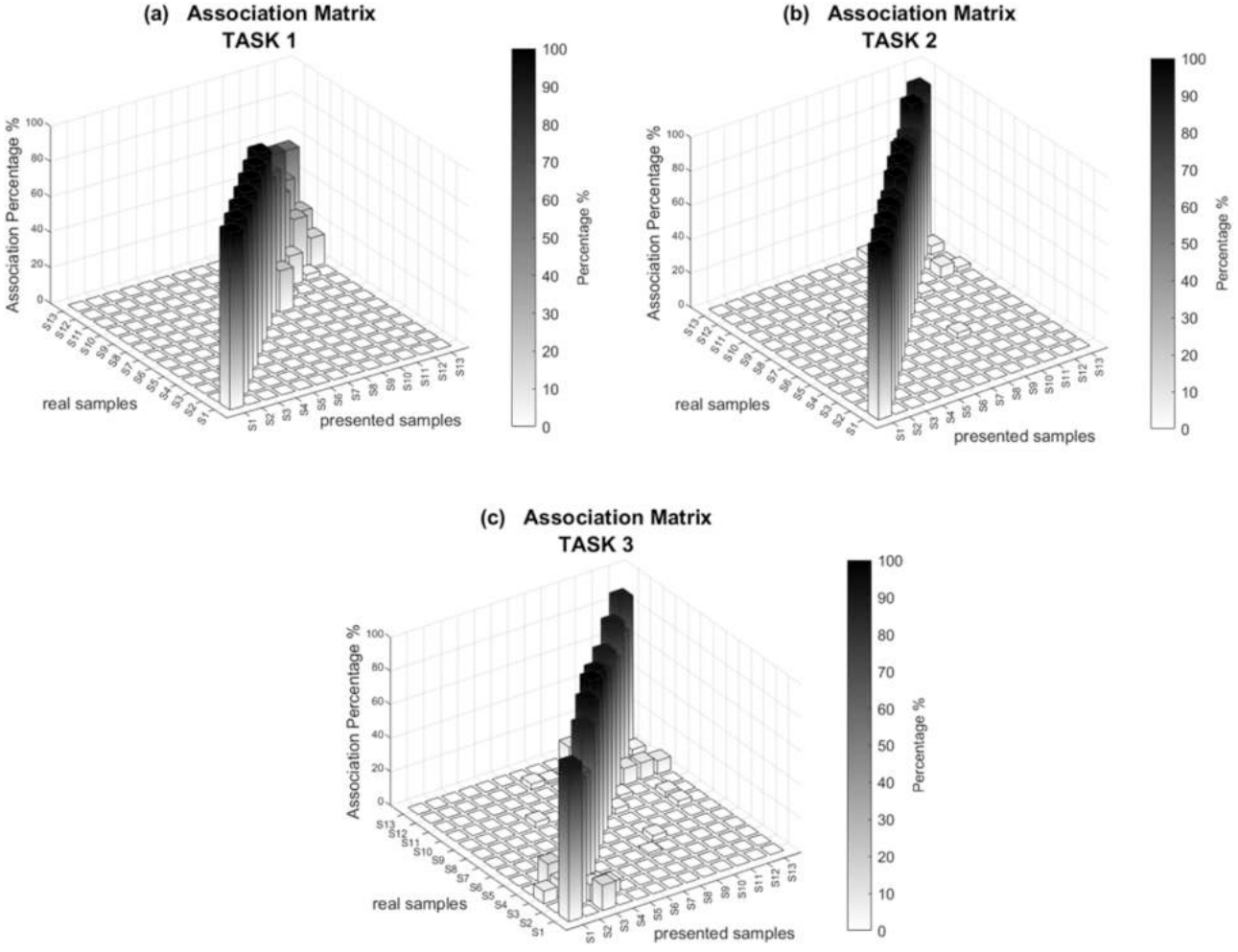

Fig. 16. Results of the discrimination campaign: (a) TASK 1, ordering of the full set of real surfaces; (b) TASK 2, discrimination task on sets of real surfaces; (c) TASK 3, discrimination task on simulated surfaces.

the excellent performance in the discrimination of both real and simulated surfaces, simulated using the PIEZOTACT device with the average transfer function. The participants have been able to correctly discriminate the real and simulated textures with few errors. This means that the simulation of the surface textures by the PIEZOTACT device using the average transfer function among participants has provided excellent results in terms of discrimination of the surfaces, and the approach is therefore validated. Moreover, it should be remarked that the panel of participants used for calculating the average transfer function (see Section 2.4) was different from the one used for the discrimination tasks, further validating the possibility to use a mean transfer function, previously calculated on an arbitrary panel of participants, for mimicking the FIV stimuli by the vibrotactile device.

The results of the discrimination campaign with the average transfer function among participants can be as well compared with those obtained from the discrimination campaign in [31], in which the simulated textures were obtained using the specific transfer function of the participants. The used discrimination protocol is exactly the same, allowing comparison between the two works. The discrimination campaigns, both of real and simulated textures, have comparably excellent results in the two works. This means that the use of an average transfer function among participants is equally effective than using, for each participant, its own specific transfer function.

The possibility of using an average transfer function in the rendering of the vibrational tactile stimuli makes it possible to get rid from having to recharacterize the finger transfer function for each individual user of the device, making this technology more versatile.

4. Conclusions

With the objective of investigating the effect of the individual finger transfer function on the tactile perception of textures, an analysis of the dynamic response of the human finger, and its role in mimicking FIV stimuli, has been conducted. The used tactile device, PIEZOTACT, is based on the exploitation of the transfer function of the system constituted by the device and the user's finger, to reproduce the Friction-Induced Vibrations previously measured when exploring real surfaces in proximal direction.

The parametric analysis on the finger's transfer function revealed that the gain of the transfer function increases as the contact force between the finger and the vibrating surface increases, while the angle between the finger and the surface slightly influenced the transfer function's shape, but no significant variations were identified.

More in general, the transfer functions obtained for the different participants involved in the study (a panel of 20 subjects, 10 female and 10 males, ranging between 20 and 55 years old), under varying conditions of contact force and angle, were found to present a quite similar trend in frequency and low deviation in amplitude. An average transfer function has been then calculated among the participants and has been employed to process FIV stimuli induced by the exploration of real isotropic textures, subsequently reproduced by the PIEZOTACT device, to be directly tested in a discrimination campaign.

The discrimination campaigns of real and simulated textures were conducted using the previously calculated average transfer function, yielding excellent discrimination results, comparable to previous studies that utilized individual participant transfer functions [31].

Such results highlighted a negligible impact of the individual finger dynamic response (Transfer Function) on the simulation of the tested textures by vibrational stimuli, allowing as well to optimize the implementation of the vibrotactile device, based on the rendering of FIV stimuli, getting rid from the need for recalibration for each individual user.

Declaration of Competing Interest

The authors declare that they have no known competing financial interests or personal relationships that could have appeared to influence the work reported in this paper.

Data Availability

Data will be made available on request.

Acknowledgements

The authors thank ARKEMA-Piezotech for providing the used piezoelectric electro-active polymers for this study. This work was supported by the project COMTACT (ANR 2020-CE28–0010-03), funded by the french "Agence Nationale de la Recherche" (ANR). All participants gave their written informed consent to take part in this study, which conformed to the ethical standards set out in the Declaration of Helsinki and which was approved by the research ethics committee CERSTAPS (IRB00012476–2021-09–12-140). This work has been partially financed by Sapienza University of Rome.

Statement of originality

With this statement, the Authors declare that:

- the manuscript is an original work and sole property of the Authors and that it has not been published and is not subjected to publication in another journal;
- the manuscript contains no sources or resources other than the ones mentioned and acknowledged;
- the manuscript does not violate other copyright or proprietary right, and it does not contain any defamatory or confidential material liable to infringe any law or contractual obligation.

References

[1] Basdogan C, Giraud F, Levesque V, Choi S. A review of surface haptics: enabling tactile effects on touch surfaces. IEEE Trans Haptics 2020;vol. 13:450–70.
[2] Choi S, Kuchenbecker KJ. Vibrotactile display: perception, technology, and applications. Proc IEEE 2013;vol. 101:2093–104.
[3] Costes A, Danieau F, Argelaguet F, Guillotel P, Lécuyer A. Towards haptic images: a survey on touchscreen-based surface haptics. IEEE Trans Haptics 2020;vol. 13:530–41.
[4] Jones LA, Sarter NB. Tactile displays: guidance for their design and application. Hum Factors 2008;vol. 50:90–111.
[5] R.H. Osgouei, "Electrostatic Friction Displays to Enhance Touchscreen Experience," in Modern Applications of Electrostatics and Dielectrics, D. Xiao e K. Sankaran, A cura di, Rijeka, IntechOpen, 2020.
[6] Gueorguiev D, Vezzoli E, Mouraux A, Lemaire-Semail B, Thonnard J-L. The tactile perception of transient changes in friction. J R Soc Interface 2017;vol. 14:20170641.
[7] Messaoud WB, Bueno M-A, Lemaire-Semail B. Relation between human perceived friction and finger friction characteristics. Tribology Int 2016;vol. 98:261–9.
[8] Torres DA, Kaci A, Giraud F, Giraud-Audine C, Amberg M, Clenet S, et al. PCA model of fundamental acoustic finger force for out-of-plane ultrasonic vibration and its correlation with friction reduction. IEEE Trans haptics 2021;vol. 14:551–63.
[9] Bueno M-A, Lemaire-Semail B, Amberg M, Giraud F. A simulation from a tactile device to render the touch of textile fabrics: a preliminary study on velvet. Text Res J 2014;vol. 84:1428–40.
[10] Camillieri B, Bueno M-A, Fabre M, Juan B, Lemaire-Semail B, Mouchnino L. From finger friction and induced vibrations to brain activation: Tactile comparison between real and virtual textile fabrics. Tribology Int 2018;vol. 126:283–96.
[11] Wiertlewski M, Friesen RF, Colgate JE. Partial squeeze film levitation modulates fingertip friction. Proc Natl Acad Sci 2016;vol. 113:9210–5.
[12] Watanabe T, Fukui S. A method for controlling tactile sensation of surface roughness using ultrasonic vibration. Proc 1995 IEEE Int Conf Robot Autom 1995.
[13] Basdogan C, Sormoli MRA, Sirin O. Modeling sliding friction between human finger and touchscreen under electroadhesion. IEEE Trans haptics 2020;vol. 13:511–21.
[14] Jiao J, Zhang Y, Wang D, Visell Y, Cao D, Guo X, et al. Data-driven rendering of fabric textures on electrostatic tactile displays. 2018 IEEE HAPTICS Symp (HAPTICS) 2018.
[15] Osgouei RH, Kim JR, Choi S. Data-driven texture modeling and rendering on electrovibration display. IEEE Trans Haptics 2020;vol. 13:298–311.

[16] Osgouei RH, Shin S, Kim JR, Choi S. An inverse neural network model for data-driven texture rendering on electrovibration display. 2018 IEEE HAPTICS Symp (HAPTICS) 2018.
[17] Vodlak T, Vidrih Z, Vezzoli E, Lemaire-Semail B, Peric D. Multi-physics modelling and experimental validation of electrovibration based haptic devices. Biotribology 2016;vol. 8:12–25.
[18] Wu S, Sun X, Wang Q, Chen J. Tactile modeling and rendering image-textures based on electrovibration. Vis Comput 2017;vol. 33:637–46.
[19] Asano S, Okamoto S, Matsuura Y, Nagano H, Yamada Y. Vibrotactile display approach that modifies roughness sensations of real textures. 2012 IEEE RO-MAN: 21st IEEE Int Symp Robot Hum Interact Commun 2012.
[20] Okamura AM, Dennerlein JT, Howe RD. Vibration feedback models for virtual environments. Proc 1998 IEEE Int Conf Robot Autom (Cat No 98CH36146) 1998.
[21] Strohmeier P, Hornbæk K. Generating haptic textures with a vibrotactile actuator. Proc 2017 CHI Conf Hum Factors Comput Syst 2017.
[22] Guruswamy VL, Lang J, Lee W-S. IIR filter models of haptic vibration textures. IEEE Trans Instrum Meas 2011;vol. 60:93–103.
[23] Romano JM, Kuchenbecker KJ. Creating realistic virtual textures from contact acceleration data. IEEE Trans Haptics 2012;vol. 5:109–19.
[24] Culbertson H, Kuchenbecker KJ. Importance of matching physical friction, hardness, and texture in creating realistic haptic virtual surfaces (January) EEE Trans Haptics 2017;vol. 10:63–74 (January).
[25] Ryu S, Pyo D, Lim S-C, Kwon D-S. Mechanical vibration influences the perception of electrovibration. Sci Rep 2018;vol. 8:4555.
[26] Liu G, Zhang C, Sun X. Tri-modal tactile display and its application into tactile perception of visualized surfaces (vol. PP) IEEE Trans Haptics 2020.
[27] Culbertson H, Unwin J, Kuchenbecker KJ. Modeling and rendering realistic textures from unconstrained tool-surface interactions. IEEE Trans haptics 2014;vol. 7:381–93.
[28] Nai W, Liu J, Sun C, Wang Q, Liu G, Sun X. Vibrotactile feedback rendering of patterned textures using a waveform segment table method. IEEE Trans Haptics 2021;vol. 14:849–61.
[29] M. Wiertlewski, D. Leonardis, D.J. Meyer, M.A. Peshkin and J.E. Colgate, "A High-Fidelity Surface-Haptic Device for Texture Rendering on Bare Finger," in *Haptics: Neuroscience, Devices, Modeling, and Applications*, Berlin, 2014.
[30] Felicetti L, Chatelet E, Latour A, Cornuault P-H, Massi F. Tactile rendering of textures by an Electro-Active Polymer piezoelectric device: mimicking Friction-Induced Vibrations. Biotribology 2022;vol. 31:100211.
[31] Felicetti L, Sutter C, Chatelet E, Latour A, Mouchnino L, Massi F. Tactile discrimination of real and simulated isotropic textures by Friction-Induced Vibrations. Tribology Int 2023;vol. 184:108443.
[32] Knez L, Slavič J, Boltežar M, et al. A sequential approach to the biodynamic modeling of a human finger. Shock Vib 2017;vol. 2017.
[33] Jindrich DL, Zhou Y, Becker T, Dennerlein JT. Non-linear viscoelastic models predict fingertip pulp force-displacement characteristics during voluntary tapping. J Biomech 2003;vol. 36:497–503.
[34] Di Bartolomeo M, Morelli F, Tonazzi D, Massi F, Berthier Y. Investigation of the role of contact-induced vibrations in tactile discrimination of textures. Mech Ind 2017;vol. 18:404.
[35] Sato S, Okamoto S, Matsuura Y, Yamada Y. Wearable finger pad deformation sensor for tactile textures in frequency domain by using accelerometer on finger side. Robomech J 2017;vol. 4:1–11.
[36] Rostamian B, Koolani M, Abdollahzade P, Lankarany M, Falotico E, Amiri M, et al. Texture recognition based on multi-sensory integration of proprioceptive and tactile signals. Sci Rep 2022;vol. 12:21690.
[37] Katz D, Krueger LE. The World of Touch. Psychology press; 2013.
[38] Roberts RD, Loomes AR, Allen HA, Di Luca M, Wing AM. Contact forces in roughness discrimination. Sci Rep 2020;vol. 10:5108.
[39] Hollins M, Risner SR. Evidence for the duplex theory of tactile texture perception. Percept Psychophys 2000;vol. 62:695–705.
[40] Faucheu J, Weiland B, Juganaru-Mathieu M, Witt A, Cornuault P-H. Tactile aesthetics: Textures that we like or hate to touch. Acta Psychol 2019;vol. 201:102950.
[41] Massimiani V, Weiland B, Chatelet E, Cornuault P-H, Faucheu J, Massi F. The role of mechanical stimuli on hedonistic and topographical discrimination of textures. Tribology Int 2020;vol. 143:106082.
[42] Cesini I, Ndengue JD, Chatelet E, Faucheu J, Massi F. Correlation between friction-induced vibrations and tactile perception during exploration tasks of isotropic and periodic textures. Tribology Int 2018;vol. 120:330–9.
[43] Hu J, Zhang X, Yang X, Jiang R, Ding X, Wang R. Analysis of fingertip/fabric friction-induced vibration signals toward vibrotactile rendering. J Text Inst 2016;vol. 107:967–75.
[44] Jiang R, Hu J, Yang X, Ding X. Analysis of fingertip/textile friction-induced vibration by time-frequency method. Fibers Polym 2016;vol. 17:630–6.
[45] Koç İM, Aksu C. Tactile sensing of constructional differences in fabrics with a polymeric finger tip. Tribology Int 2013;vol. 59:339–49.
[46] Fagiani R, Massi F, Chatelet E, Berthier Y, Akay A. Tactile perception by friction induced vibrations. Tribology Int 2011;vol. 44:1100–10.
[47] Fagiani R, Massi F, Chatelet E, Berthier Y, Sestieri A. Experimental analysis of friction-induced vibrations at the finger contact surface. Proc Inst Mech Eng, Part J: J Eng Tribology 2010;vol. 224:1027–35.
[48] Greenspon CM, McLellan KR, Lieber JD, Bensmaia SJ. Effect of scanning speed on texture-elicited vibrations. J R Soc Interface 2020;vol. 17:20190892.
[49] Dacleu Ndengue J, Cesini I, Faucheu J, Chatelet E, Zahouani H, Delafosse D, et al. Tactile perception and friction-induced vibrations: discrimination of similarly patterned wood-like surfaces. IEEE Trans Haptics 2017;vol. 10:409–17.
[50] Lacerra G, Di Bartolomeo M, Milana S, Baillet L, Chatelet E, Massi F. Validation of a new frictional law for simulating friction-induced vibrations of rough surfaces. Tribology Int 2018;vol. 121:468–80.
[51] Zhou X, Mo JL, Li YY, Xu JY, Zhang X, Cai S, et al. Correlation between tactile perception and tribological and dynamical properties for human finger under different sliding speeds. Tribology Int 2018;vol. 123:286–95.
[52] Zhou X, Mo JL, Li YY, Xiang ZY, Yang D, Masen MA, et al. Effect of finger sliding direction on tactile perception, friction and dynamics. Tribology Lett 2020;vol. 68:1–13.
[53] Prevost A, Scheibert J, Debrégeas G. Effect of fingerprints orientation on skin vibrations during tactile exploration of textured surfaces. Commun Integr Biol 2009;vol. 2:422–4.
[54] Kuroki S, Watanabe J, Nishida S. Integration of vibrotactile frequency information beyond the mechanoreceptor channel and somatotopy. Sci Rep 2017;vol. 7:2758.
[55] Sutter C, Moinon A, Felicetti L, Massi F, Blouin J, Mouchnino L. "Cortical facilitation of tactile afferents during the preparation of a body weight transfer when standing on a biomimetic surface. Front Neurol 2023;vol. 14:1175667.
[56] Özgün N, Strauss DJ, Bennewitz R. Tribology of a braille display and EEG correlates. Tribology Lett 2018;vol. 66:1–10.